Polar Geosci., **14**, 39–52, 2001

Experimental constraints on partial melting under UHT and dry conditions of quartzo-feldspathic rock in the Napier Complex, East Antarctica

Tomokazu Hokada[1,*] and Makoto Arima[2]

[1]*National Institute of Polar Research, Kaga 1-chome, Itabashi-ku, Tokyo 173-8515*
[2]*Department of Environmental Sciences, Yokohama National University, Tokiwadai, Hodogaya-ku, Yokohama 240-8501*

Abstract: We carried out high pressure melting experiments on a mixture of mineral separates of quartz, plagioclase (antiperthite) and a rare amount of orthopyroxene at 1000–1150°C and 1.0 GPa under dry conditions. The starting material was obtained from an ultrahigh-temperature (UHT) garnet-orthopyroxene-bearing quartzo-feldspathic gneiss in the Mt. Riiser-Larsen of the Napier Complex, East Antarctica. This UHT gneiss is considered to be equilibrated at metamorphic conditions >1070°C. The mineral assemblages in the run products at 1000°C and 1100°C are the same as those of the starting material. K_2O content in K-feldspar lamellae of antiperthite decreases with temperature. Granitic glass (<10 vol%) was detected along boundaries between lamella-free plagioclase and quartz grains in the run at 1150°C.

The experimental results indicate that the homogenization temperature of this antiperthite lies <1150°C at 1.0 GPa. It is consistent with the estimated temperature from feldspar geothermometry. Major element composition of the glass at 1150°C shows the molecular $Al_2O_3/(Na_2O+K_2O+CaO)$ ratio (A.S.I.: aluminum saturation index)=1.08 and high Na_2O+K_2O contents (8.1 wt%) relative to low CaO (1.3 wt%), which is comparable to the chemical features of A-type granite or leucogranite. This may imply that some genetic links might exist between UHT metamorphism and A-type granite magmatism in the Napier Complex.

key words: dry condition, feldspar, melting experiment, Napier Complex, ultrahigh-temperature (UHT) metamorphism

1. Introduction

Partial melting of crustal rocks and subsequent segregation of the melt lead to chemical differentiation of the deep crust. Such processes are commonly associated with high-temperature metamorphism, and the segregated melts form igneous bodies that are either associated with the parental metamorphic rocks or intrude into the overlying sequences. Various field and petrological features related to this have been reported from many high-grade metamorphic terrains (*e.g.*, Atherton and Gribble, 1983; Ashworth and Brown, 1990; Brown, 1994). The Napier Complex in East Antarctica is one such high-grade metamorphic terrain, and is known to have undergone >1000°C ultrahigh-

*Present address: Department of Geology, National Science Museum, 3-23-1 Hyakunin-cho, Shinjuku-ku, Tokyo 169-0073.

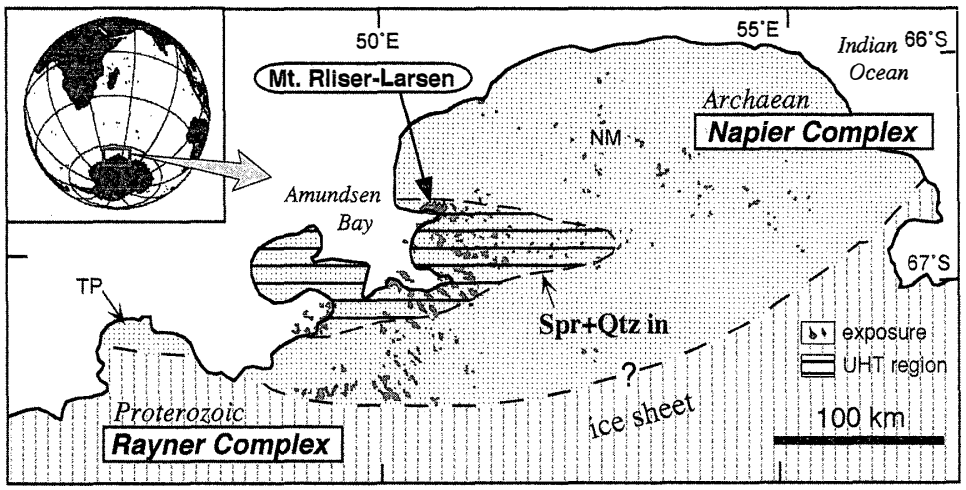

Fig. 1. Geological outline of the Napier Complex and surrounding area in East Antarctica. The estimated boundary between the Napier Complex and the Rayner Complex is after Sheraton et al. (1987). The UHT region defined by "Sapphirine+quartz (Spr+Qtz) in" isograd is taken from Harley and Hensen (1990). NM: Napier Mountains. TP: Tange Promontory.

temperature (UHT) metamorphism of regional extent (200 km × 100 km, Fig. 1; Harley and Hensen, 1990). Even though such high metamorphic temperatures have been achieved, evidence of partial melting such as migmatite or syn-metamorphic igneous intrusions is quite rare, and the layered structure composed of a variety of rock types is conspicuous in the complex (Sheraton *et al.*, 1987).

The UHT metamorphic rocks in the Napier Complex are characterized by anhydrous peak mineral assemblages with minor amounts of hydrous minerals (*e.g.*, Sheraton *et al.*, 1987). Most of the hydrous minerals are obviously retrograde products on the basis of their modes of occurrence. Some of biotite and amphibole in the UHT gneisses are possibly prograde phases, considered to be stabilized by high fluorine or chlorine components in place of H_2O (or OH) within their crystal structures (Hensen and Osanai, 1994; Tsunogae *et al.*, 2000; Motoyoshi and Hensen, 2001). It is, therefore, likely that the lack of H_2O-bearing phases in UHT gneisses prevents a high percentage of melting even at such high metamorphic temperatures. Localized partial melting during UHT metamorphism is occasionally implied by field and petrological observations in the Napier Complex (*e.g.*, Sheraton *et al.*, 1987; Grew, 1998; Osanai *et al.*, 1999; Hokada *et al.*, 1999; Yoshimura *et al.*, 2000). Grew *et al.* (2000) suggested that beryllium pegmatites in the Napier Complex were formed by melting of sapphirine-bearing metapelites during the UHT metamorphism. In addition, several large granitic intrusions are reported from a few localities at relatively lower-grade areas in the complex (*e.g.*, Napier Mountains and Tange Promontory, Fig. 1; Sheraton *et al.*, 1987). However, the genetic relations of these igneous rocks to the UHT metamorphism are less evident.

In the Mt. Riiser-Larsen area of the UHT region of the Napier Complex (Harley and Hensen, 1990; Ishizuka *et al.*, 1998), leucocratic veins or patches are occasionally observed. We consider that they were possibly formed by partial melting of UHT metamorphic rocks. To assess the possibility of melting during UHT metamorphism, we have carried out melting experiments under UHT and dry conditions using a quartzo-

feldspathic gneiss from Mt. Riiser-Larsen. Experimental investigations on the melt include relatively large chemical variations, because multiple components are incorporated into the melt. This study focuses on the relatively simple quartz-feldspar system, but expands into ternary feldspar in addition to the quartz-albite-orthoclase (haplogranite) system (*e.g.*, Johannes and Holtz, 1996).

2. Experimental procedures

2.1. Starting material

Garnet-orthopyroxene-bearing quartzo-feldspathic gneiss (sp. R98022301A) from the Mt. Riiser-Larsen area was used in the experiments. The gneiss is composed of quartz, plagioclase, garnet and orthopyroxene. Rutile, ilmenite, biotite, zircon and monazite are minor. Plagioclase in the starting material is antiperthite (Fig. 2). Hokada (1999, 2001) calculated the chemical compositions of pre-exsolution antiperthite grains (Fig. 3a), and estimated that the equilibrium temperature exceeded 1070°C by feldspar geothermometer (Fuhrman and Lindsley, 1988).

The rock sample was ground in a tungsten-carbide mortar. Quartz and feldspar grains (<250 μm) were separated by using a sieve, magnet and heavy liquid. A trace amount of orthopyroxene could not be removed by the mineral separation process. A few tiny (<50 μm) orthopyroxene grains were present in the starting mixes. The separated minerals were dried at 110°C in the oven before being loaded in a Pt capsule.

Bulk chemical composition of the starting material (Table 1) was analyzed by X-ray fluorescence analyzer (XRF: Rigaku RIX-3000) at the National Institute of Polar Research. The analytical procedure followed Motoyoshi and Shiraishi (1995). Chemical compositions of the minerals used in the experiments (Table 2) were determined by using an electron microprobe with an wavelength dispersive spectrometry (WDS: JEOL-JXA8800) at the National Institute of Polar Research. Analytical conditions were 15 kV

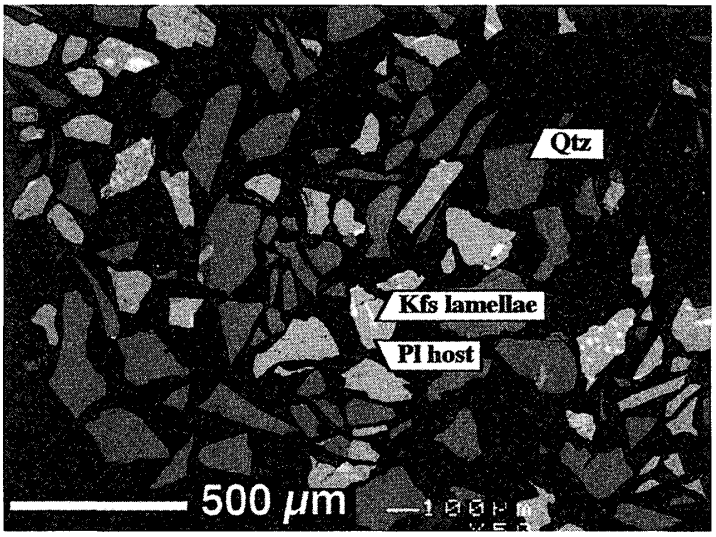

Fig. 2. Back-scattered electron image of mineral mixture of quartz (Qtz) and plagioclase (Pl) used in the present experiments as starting material. Note that Plagioclase represents antiperthitic K-feldspar (Kfs) lamellae.

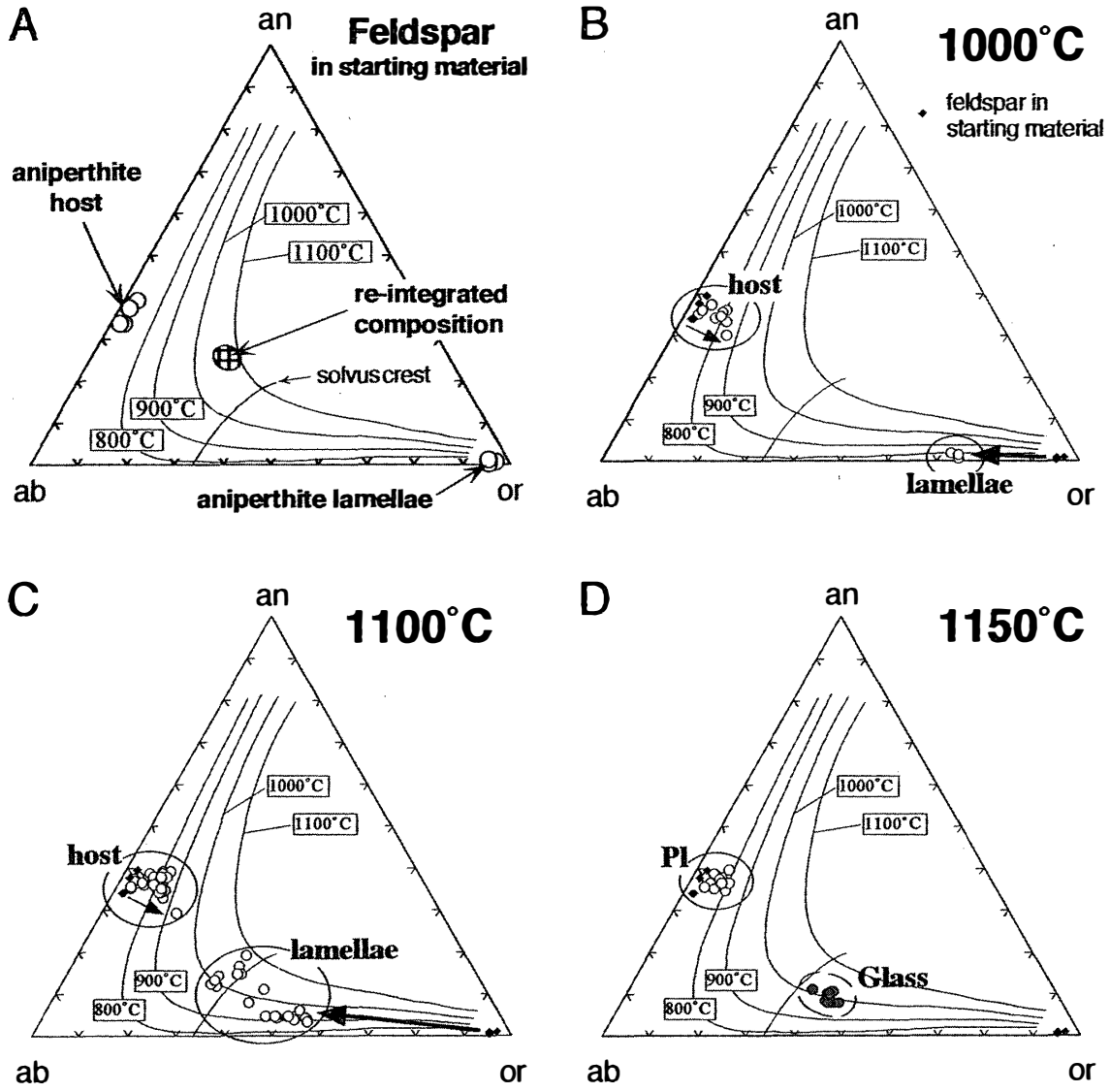

Fig. 3. Ternary plots of feldspar compositions. Isotherms are calculated for 0.8 GPa using Fuhrman and Lindsley (1988). (a) Antiperthite lamellae and host compositions along with re-integrated pre-exsolution feldspar compositions calculated by the volume proportions of the exsolution in the starting material (sp. R98022301A). (b) Feldspar compositions in the run product at 1000°C. (c) Feldspar compositions in the run product at 1100°C. (d) Feldspar and glass compositions in the run product at 1150°C. Note that antiperthitic lamellae within plagioclase are homogenized.

accelerating voltage, 8 nA probe current and 10–20 s counting time for each element with a focused <1 μm beam under which sodium is not evaporated. ZAF correction was applied and natural and synthesized oxides were used as standards of the analysis.

2.2. Experimental technique

The experiments were carried out using a 1.27 cm piston cylinder apparatus at Yokohama National University with talc-Pyrex pressure cells internal to the graphite heater sleeve. Experimental pressure was fixed at 1.0 GPa. Pressures reported are

Table 1. Bulk and CIPW NORM compositions of the starting material.

Bulk (wt %)		CIPW NORM	
SiO_2	83.31	Q	59.55
TiO_2	0.09	C	0.25
Al_2O_3	9.96	F	38.80
FeO*	0.27	an	12.90
MgO	0.28	ab	21.23
CaO	2.60	or	4.67
Na_2O	2.51	hy	1.05
K_2O	0.79	en	0.70
Total	99.81	fs	0.35
		il	0.17
		Total	99.82

* Total Fe as FeO

Table 2. Chemical compositions of minerals used as the starting material. Re-integrated pre-exsolution feldspar composition (labelled 'int') estimated by Hokada (1999, 2001) is also shown (see text for details).

(a) Pl	host	lamellae	int.	(b) Opx	
wt %				wt %	
SiO_2	60.98	64.85	62.13	SiO_2	50.66
TiO_2	0.07	0.33	0.15	TiO_2	0.21
Al_2O_3	25.17	18.49	23.19	Al_2O_3	5.49
Cr_2O_3	0.00	0.02	0.01	Cr_2O_3	0.00
Fe_2O_3*	0.00	0.08	0.02	FeO**	22.49
MnO	0.04	0.07	0.05	MnO	0.09
MgO	0.00	0.00	0.00	MgO	21.17
CaO	7.14	0.11	5.05	CaO	0.13
Na_2O	7.05	0.49	5.10	Na_2O	0.01
K_2O	0.32	15.58	4.85	K_2O	0.00
BaO	0.08	0.74	0.28		
Total	100.85	100.76	100.82	Total	100.25
cations (O=8)				cations (O=6)	
Si	2.691	2.984	2.778	Si	1.877
Ti	0.002	0.011	0.005	Ti	0.006
Al	1.309	1.003	1.218	Al	0.240
Cr	0.000	0.000	0.000	Cr	0.000
Fe	0.000	0.001	0.000	Fe	0.697
Mn	0.000	0.003	0.001	Mn	0.003
Mg	0.000	0.000	0.000	Mg	1.169
Ca	0.338	0.005	0.239	Ca	0.005
Na	0.603	0.044	0.437	Na	0.001
K	0.018	0.915	0.284	K	0.000
Ba	0.001	0.013	0.005		
Total	4.962	4.979	4.967	Total	3.998
an	0.352	0.006	0.249	X_{Mg} ***	0.626
ab	0.629	0.045	0.456	** Total Fe as FeO	
or	0.019	0.949	0.295	*** X_{Mg}: Mg/(Mg+Fe)	

* Total Fe as Fe_2O_3

nominal "piston in" values, monitored on calibrated Heise gauges, corrected by −13% friction correction. Temperatures were measured with Pt-$Pt_{87}Rh_{13}$ thermocouples, and were controlled within 10°C of reported values. A total of 10–20 mg of dried sample

was loaded into a Pt capsule without water added. No buffering material was used for oxygen fugacity control. Run durations were 235 hours (1000°C), 164 hours (1100°C) and 64 hours (1150°C).

Run products were mounted using epoxy resin and polished with diamond paste for electron microprobe analysis. These were examined under the scanning electron microscope. Major elements were analyzed by WDS at the National Institute of Polar Research.

3. Experimental results

Run conditions and the experimental results are summarized in Tables 3 and 4. Back-scattered electron images and the X-ray concentration maps of the run products are given in Figs. 4, 5, 6 and 7. The glass (quenched melt) was observed in the 1150°C run product only. Exsolution lamellae of antiperthitic plagioclase persisted in the run products at 1000°C and 1100°C, but their compositions were changed. Chemical variations of feldspars in the run products are given in Fig. 3. Exsolution lamellae were homogenized in the 1150°C run.

Trace amounts of sub-micron scale K-bearing phase were present in the products at both 1000°C and 1100°C runs (Figs. 4 and 5). These K-bearing phases might be a melt generated in the experiments, but they are too fine to confirm their compositions. Run conditions (1000°C and 1100°C) exceeded the hydrous solidus temperature (700–800°C) of the quartz-feldspar system (Johannes and Holtz, 1996). The starting material is mineral separates of natural rock; sub-micron scale hydrous phase contained as an impurity in the starting mix might generate a very trace amount of melt. We believe that such accidental and trace melt formation does not affect the phase relations of the run products. For this reason, the minor 'K-bearing phase' is ignored in the discussion of this generation of granitic melt.

At 1000°C (run No. FP-04), the mineral assemblage of the run product is the same as that of the starting material. Antiperthitic lamellae retained their shape (Fig. 4). The chemical composition of the exsolution lamellae slightly shifted to the Na-rich side of that of the starting material. The albite component in the K-feldspar lamellae of antiperthite increased from 5 mol% to 25 mol%, whereas anorthite content was constant (Fig. 3b and Table 4). The host domain of the antiperthitic feldspar showed a slight compositional zoning. Orthoclase content was 1 mol% at the core or near the lamellae-bearing portion and 9 mol% at the rim.

At 1100°C (run No. FP-05), the mineral assemblage of the run product was the same as that of the starting material. The exsolution lamellae still remained. Their shapes were not so sharp under SEM observation (Fig. 5) compared to those of the

Table 3. Run conditions and results.

Run No.	T (°C)	duration (h)	Melt	Lamellae
FP-04	1000	235	not generated *	persist
FP-05	1100	164	not generated *	persist
FP-02	1150	57	generated	disappeared

* Trace amount of melt might be generated locally (see text for details).

Table 4. Representative electron microprobe analyses of the run products.

(a) Pl	FP-04 - 1000°C		FP-05 - 1100°C		FP-02 -
	host	lamellae	host	lamellae	1150°C
wt %					
SiO_2	59.55	65.87	58.93	64.50	60.02
TiO_2	0.02	0.07	0.00	0.21	0.00
Al_2O_3	25.04	19.08	24.95	19.65	25.07
Cr_2O_3	0.06	0.00	0.01	0.01	0.00
Fe_2O_3*	0.18	0.02	0.20	0.12	0.07
MnO	0.01	0.00	0.04	0.11	0.00
MgO	0.08	0.00	0.03	0.00	0.03
CaO	6.98	0.35	7.27	1.29	7.30
Na_2O	6.59	2.77	6.30	4.57	6.30
K_2O	1.07	12.41	1.55	8.72	1.01
BaO	0.16	0.13	0.00	0.10	0.04
Total	99.74	100.70	99.28	99.28	99.84
cations (O=8)					
Si	2.671	2.984	2.662	2.937	2.682
Ti	0.001	0.002	0.000	0.007	0.000
Al	1.324	1.019	1.328	1.055	1.320
Cr	0.002	0.000	0.000	0.000	0.000
Fe	0.006	0.001	0.007	0.004	0.002
Mn	0.000	0.000	0.002	0.004	0.000
Mg	0.005	0.000	0.002	0.000	0.002
Ca	0.335	0.017	0.352	0.063	0.349
Na	0.573	0.243	0.551	0.403	0.548
K	0.061	0.717	0.089	0.507	0.057
Ba	0.003	0.002	0.000	0.002	0.001
Total	4.981	4.985	4.993	4.982	4.961
an	0.346	0.017	0.355	0.065	0.366
ab	0.591	0.249	0.555	0.414	0.574
or	0.063	0.734	0.090	0.521	0.060

* Total Fe as Fe_2O_3

(b) Opx	FP-02 - 1150°C
wt %	
SiO_2	50.42
TiO_2	0.15
Al_2O_3	5.90
Cr_2O_3	0.07
FeO**	22.37
MnO	0.04
MgO	21.31
CaO	0.18
Na_2O	0.08
K_2O	0.00
Total	100.52
cations (O=6)	
Si	1.862
Ti	0.004
Al	0.257
Cr	0.002
Fe	0.691
Mn	0.001
Mg	1.173
Ca	0.007
Na	0.006
K	0.000
Total	4.003
X_{Mg} ***	0.629

** Total Fe as FeO

*** X_{Mg}: Mg/(Mg+Fe)

(c) Melt	FP-02 - 1150°C	
	average	1 sigma
wt %	(n=13)	
SiO_2	73.31	0.61
TiO_2	0.40	0.37
Al_2O_3	14.04	0.32
Cr_2O_3	0.03	0.04
FeO**	1.24	0.19
MnO	0.03	0.04
MgO	0.85	0.09
CaO	1.26	0.18
Na_2O	3.46	0.19
K_2O	4.61	0.07
BaO	0.66	0.61
Total	99.89	0.85
CIPW NORM (wt %)		
Q	30.84	
C	1.07	
F	62.78	
an	6.25	
ab	29.27	
or	27.26	
hy	3.73	
en	2.12	
fs	1.61	
il	0.76	
Total	99.18	
(molecular)		
X_{Mg} ***	0.55	
A.S.I †	1.08	

† A.S.I.: aluminum saturation index (molecular Al_2O_3/Na_2O+K_2O+CaO)

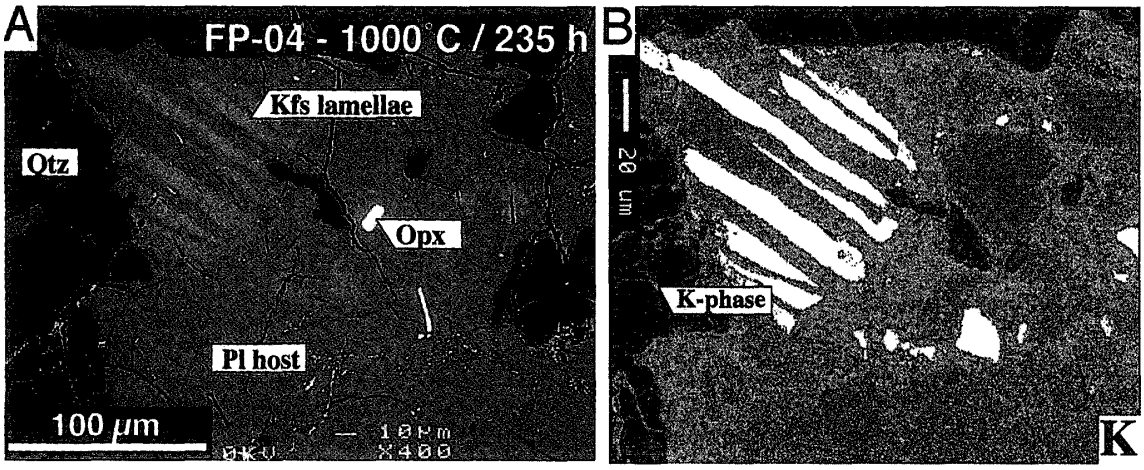

Fig. 4. (a) Back-scattered electron image of the run product at 1000°C. (b) Potassium X-ray concentration map of the same area as shown in (a). Sub-micron scale K-bearing phase (labeled 'K-phase') is found. See text for details. Opx: orthopyroxene.

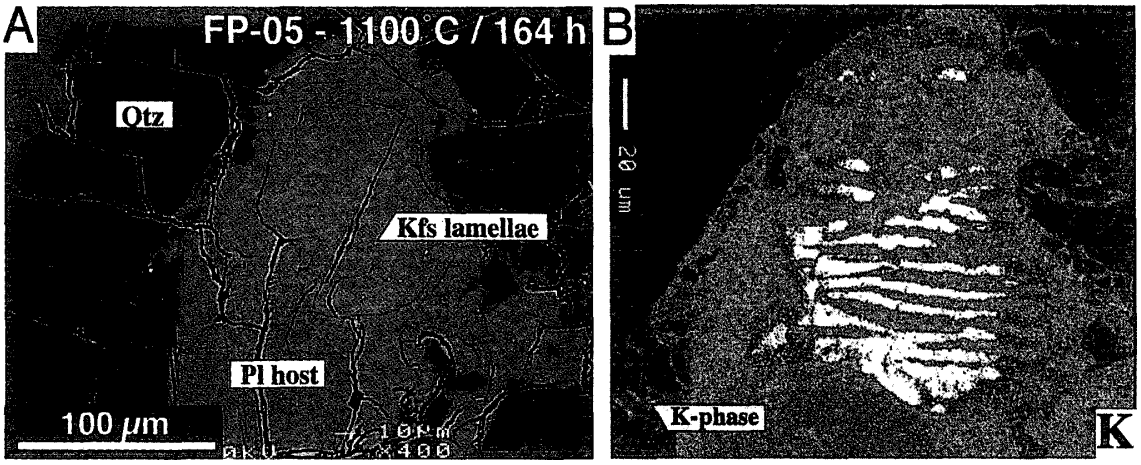

Fig. 5. (a) Back-scattered electron image of the run product at 1100°C. (b) Potassium X-ray concentration map of the same area as shown in (a). Sub-micron scale K-bearing phase is observed.

original and the 1000°C lamellae. Chemical compositions of the lamellae were greatly modified; the albite component in the K-feldspar lamellae of antiperthite increased from 5 mol% to 55 mol% with anorthite content slightly increasing from 1 mol% to 7 mol% (Fig. 3c and Table 4). Compositional zoning within the host domain of the antiperthite was observed, from orthoclase content of 3 mol% in the core or near the lamellae-bearing portion to 7 mol% at the rim.

At 1150°C (run No. FP-02), granitic glass (<10 vol%) was generated along boundaries between quartz and feldspar grains (Figs. 6 and 7). The glass is chemically homogeneous and slightly Na-poorer than the water-saturated eutectic minimum of haplogranite system (Fig. 3d and Table 4). The total wt% (almost 100 wt%) of the glass analyses indicates that the generated melt was almost anhydrous and the dry melting took place at this condition. Aggregates of fine and idiomorphic orthopyroxene grains, <5 μm in diameter, were locally present in the glass (Figs. 6b and 7). These orthopyroxenes are

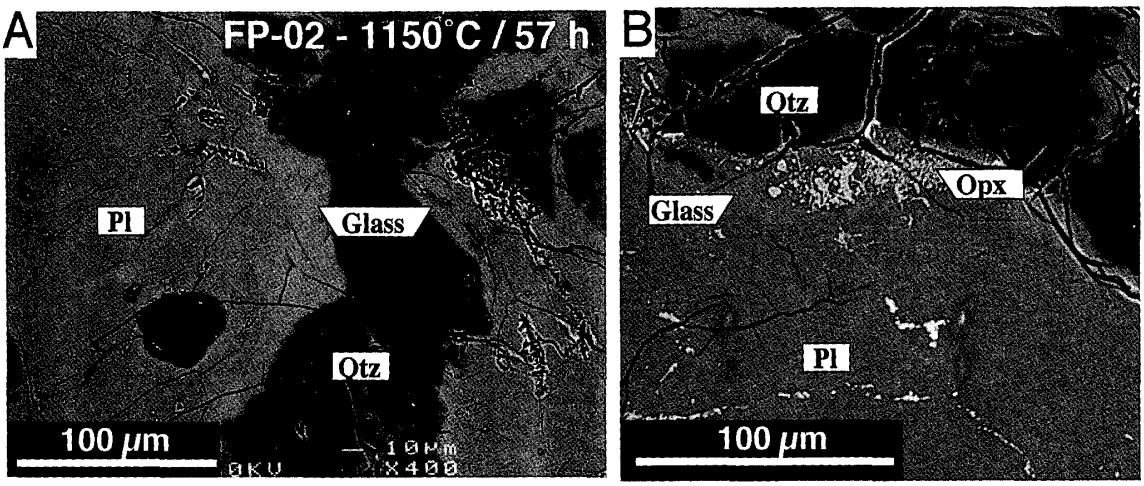

Fig. 6. Back-scattered electron images of the run product at 1150°C. (a) Granitic glass is observed along boundaries between feldspar and quartz grains. (b) Fine-grained and euhedral orthopyroxene grains are observed in the glass.

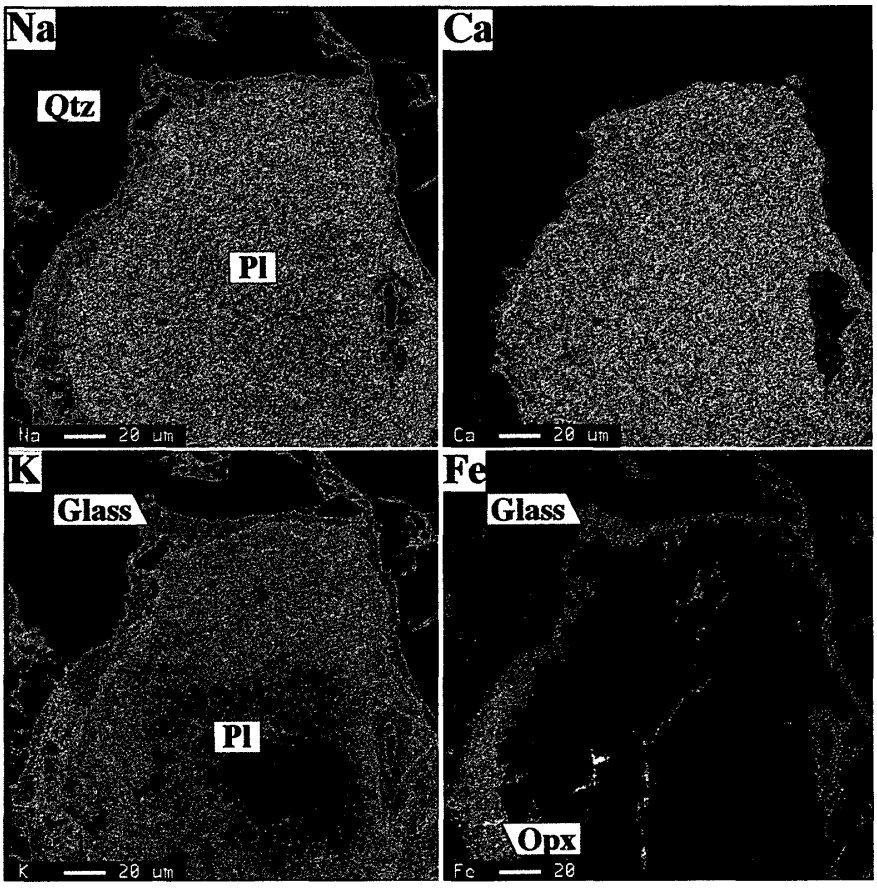

Fig. 7. X-ray concentration maps of the run product at 1150°C. Warmer colors represent higher concentrations.

considered to have been formed during the melting, and showed similar compositions to those in the starting material. Exsolution lamellae within plagioclase crystals were homogenized.

4. Discussion and conclusions

4.1. Partial melting of quartz-feldspar system under UHT and dry conditions

Our results suggest that the dry solidus of the mineral mix of quartz and feldspar from the UHT gneiss lies between 1100°C and 1150°C, which is close to the peak metamorphic temperatures attained in the study area (>1100–1120°C; Harley and Motoyoshi, 2000; Hokada, 1999, 2001). A number of experimental investigations concerning the generation of granitic melt have been reported (Johannes and Holtz, 1996; and see references therein). However, most of these targeted water-present and amphibolite-granulite facies conditions, and few attempts have been made to determine

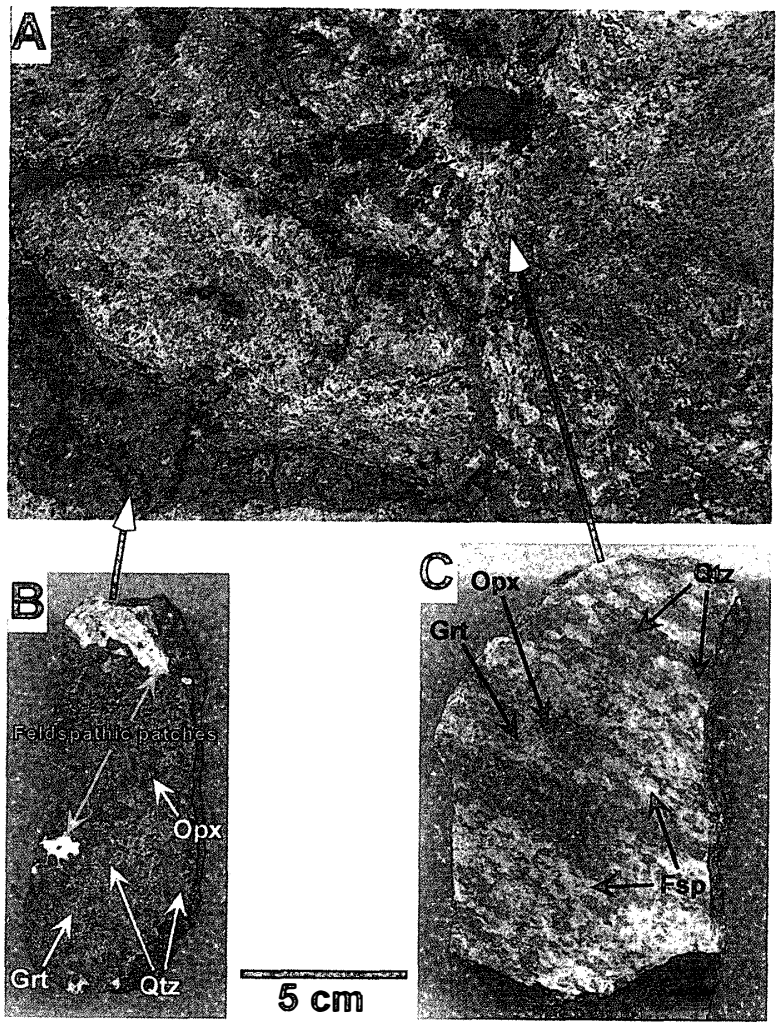

Fig. 8. Field photograph of the sample used in the experiments. (a) Layered structure of garnet-orthopyroxene gneisses is disturbed around the sample localities. (b) Feldspathic patches or veins are conspicuous in the siliceous domain of the gneisses. (c) Heterogeneous garnet-orthopyroxene-bearing quartzo-feldspathic gneiss used for the experiments (sp. R98022301A). Grt: garnet. Fsp: feldspar.

dry melting under UHT conditions. Johannes and Holtz (1996) noted that the dry solidus of the quartz-albite-orthoclase (haplogranite) system lies at around 1050°C at 1 GPa. Whitney (1975) carried out melting experiments using quartz-albite-orthoclase-anorthite (ternary feldspar) components in addition to the haplogranite system, and estimated 1100–1200°C for the dry solidus at 0.8 GPa, although they did not present compositions of the generated glass. Thus, our experimental results are the first to show quantitative data for melting in a quartz-ternary feldspar system under UHT and dry conditions.

The UHT quartzo-feldspathic gneiss used for the experiments occurs in heterogeneous layers where the layered structure is disturbed and feldspathic veins or patches are locally present, especially in the siliceous domain of the gneisses (Fig. 8). These field observations suggest that partial melting may take place in quartzo-feldspathic rocks under UHT and dry conditions. Nevertheless, our study does not imply that dry melting was of regional extent during the UHT metamorphism. Mineral assemblages of quartz+plagioclase (antiperthite)+orthopyroxene are common in felsic or quartzo-feldspathic gneisses in the Napier Complex, and it is possible that partial melting may have occurred more extensively. The evidence of melting would be obliterated by deformation during the cooling stage or by back reaction to crystallize high temperature minerals from the melt.

The starting material of our experiments contained a trace amount (<1%) of orthopyroxene (and other phases). The effect of these additional phases was ignored because of their small quantities, although further study to assess them is needed. The silica content of the starting material was high (SiO_2=83 wt%) compared with typical granitic rocks. This was probably due to the selective removal of feldspar grains from

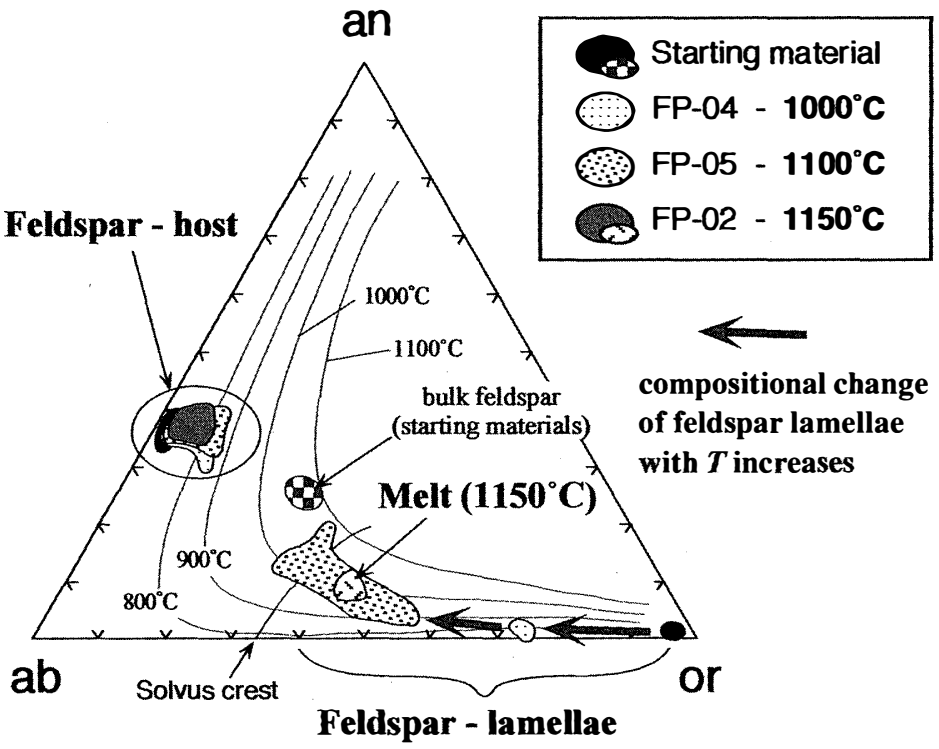

Fig. 9. Summary of the chemical variations of feldspars and melt in the experimental results.

the starting material during sample preparation, especially by heavy liquid separation. The glass formed in the run product at 1150°C is restricted to occur along boundaries between quartz and feldspar grains. This indicates that eutectic-like melting occurs in the quartz-feldspar system, and that the effect of the relatively high silica (quartz) content in the starting material is probably not so essential.

The homogenization temperature of antiperthite (between 1100°C and 1150°C) estimated here is comparable to the metamorphic temperature obtained by feldspar geothermometry for the same sample (Hokada, 1999, 2001). However, homogenized feldspar composition is not really the same as in the estimated pre-exsolution compositions of the feldspar in the gneiss (Fig. 3). This is probably because the K_2O component in plagioclase would be selectively incorporated into the coexisting melt at 1150°C, and actual homogenization temperature would be lower than this. We noted systematic chemical and morphological variations of the K-feldspar lamellae in the plagioclase; K_2O content in the lamellae decreases with temperature (Fig. 9). However, the chemical compositions of the antiperthite host do not lie on the calculated isotherms of ternary feldspar (Figs. 3 and 9); and compositional zoning of the feldspar was observed in the run at 1000°C and 1100°C. These probably reflect the low diffusion rate within the feldspar crystal. Further experiments of longer duration or reversal experiments are needed to quantify the accurate homogenization temperature of this feldspar.

4.2. Implications for granitic magmatism of the Napier Complex

Chemical compositions of the glass generated in the run product at 1150°C show the molecular $Al_2O_3/(Na_2O+K_2O+CaO)$ ratio (A.S.I.: aluminum saturation index)=1.08 and high Na_2O+K_2O contents (8.1 wt%) relative to low CaO (1.3 wt%) (Table 4), which is

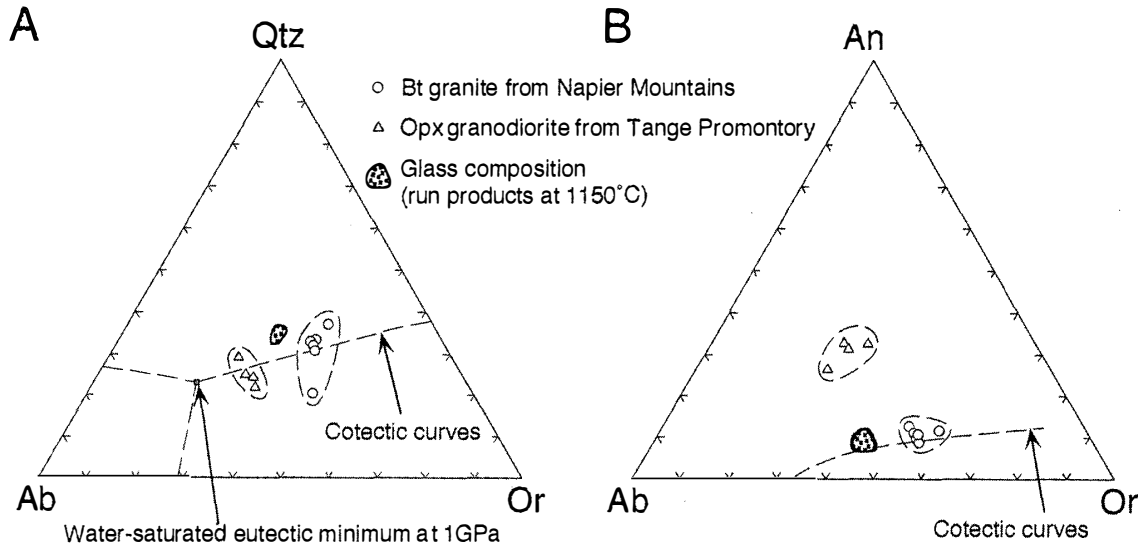

Fig. 10. Comparison of the glass compositions in the run product at 1150°C to the chemistry of the granitic rocks reported from the Napier Complex (Sheraton et al., 1987). (a) Quartz-albite-orthoclase ternary plots. Eutectic and cotectic compositions for water-saturated system at 1 GPa are after Johannes and Holtz (1996). (b) Anorthite-albite-orthoclase ternary plots.

comparable to the chemical features of A-type granites or leucogranites (Collins *et al.*, 1982; Whalen *et al.*, 1987; Johannes and Holtz, 1996). In the northern (Napier Mountains) and western (Tange Promontory) areas of the Napier Complex, several syn-metamorphic granitic intrusions have been reported; chemical features of these rocks also represent those of A-type granites (Sheraton *et al.*, 1987). Ternary plots of the glass composition in the run product at 1150°C are somewhat similar to those of the bulk compositions of the biotite granites in the Napier Mountains (Fig. 10). Although the experimental results presented here are not directly applicable to formation of granitic rocks in the complex, the result presented here might imply that genetic links may exist between the ultrahigh-temperature metamorphic rocks and the A-type granites in the Napier Complex.

High temperatures >900°C and low-water and high-fluorine or chlorine contents in the magmas have been suggested by experimental investigations of A-type granites (Clemens *et al.*, 1986; Skjerlie and Johnston, 1992; Patiño Douce, 1997). Such high temperature regimes are comparable to the category of UHT metamorphism, which is also defined as >900°C crustal metamorphism (Harley, 1998). The presence of high-fluorine and chlorine minerals in the UHT metamorphic rocks of the Napier Complex (*e.g.*, Tsunogae *et al.*, 2000; Motoyoshi and Hensen, 2001) also implies that the formation of A-type granites may be related to the partial melting associated with the UHT metamorphism under relatively dry conditions, although further experimental and petrological studies are needed to assess this idea.

Acknowledgments

Professors T. Kawasaki and S.L. Harley reviewed the manuscript. We appreciate their thoughtful and critical comments, which much improved the paper. This work was financially supported by the Sasakawa Scientific Research Grant from The Japan Science Society to T.H. and by a Grant-in-Aid from the Ministry of Science, Sports and Culture, Japan, to M.A. (no. 08454154).

References

Ashworth, J.R. and Brown, M. (1990): Migmatites, Melting and Metamorphism. London, Unwin Hyman, 407 p.

Atherton, M.P. and Gribble, C.D. (1983): Migmatites, Melting and Metamorphism. Nantwich, Shiva Publishing, 326 p.

Brown, M. (1994): The generation, segregation, ascent and emplacement of granitic magma: the migmatite-to-crustally-derived granite connection in thickened orogens. Earth-Sci. Rev., **36**, 83–130.

Clemens, J.D., Holloway, J.R. and White, A.J.R. (1986): Origin of an A-type granite: experimental constraints. Am. Mineral., **71**, 317–324.

Collins, W.J., Beams, S.D., White, A.J.R. and Chappell, B.W. (1982): Nature and origin of A-type Granites with particular reference to Southeastern Australia. Contrib. Mineral. Petrol., **80**, 189–200.

Fuhrman, M.L. and Lindsley, D.H. (1988) Ternary-feldspar modeling and thermometry. Am. Mineral., **73**, 201–215.

Grew, E.S. (1998): Boron and beryllium minerals in granulite-facies pegmatites and implications of beryllium pegmatites for the origin and evolution of the Archean Napier Complex of East

Antarctica. Mem. Natl Inst. Polar Res., Spec. Issue, **53**, 74–92.
Grew, E.S., Martin, G.Y., Barbier, J., Shearer, C.K., Sheraton, J.W., Shiraishi, K. and Motoyoshi, Y. (2000): Granulite-facies beryllium pegmatites in the Napier Complex in Khmara and Amundsen Bays, western Enderby Land, East Antarctica. Polar Geosci., **13**, 1–40.
Harley, S.L. (1998): On the occurrence and characterization of ultrahigh-temperature crustal metamorphism. What Drives Metamorphism and Metamorphic Reactions?, ed. by P.J. Treloar and P. O'Brien. London, Geol. Soc., 81–107.
Harley, S.L. and Hensen, B.J. (1990): Archaean and Proterozoic high-grade terranes of East Antarctica (40–80°E): a case study of diversity in granulite facies metamorphism. High-temperature Metamorphism and Crustal Anatexis, ed. by J.R. Ashworth and M. Brown. London, Unwin Hyman, 320–370.
Harley, S.L. and Motoyoshi, Y. (2000): Al zoning in orthopyroxene in a sapphirine quartzite: evidence for >1120°C UHT metamorphism in the Napier Complex, Antarctica, and implications for the entropy of sapphirine. Contrib. Mineral. Petrol., **138**, 293–307.
Hensen, B.J. and Osanai, Y. (1994): Experimental study of dehydration melting of F-bearing biotite in model pelitic compositions. Mineral. Mag., **58A**, 410–411.
Hokada, T. (1999): Thermal evolution of the ultrahigh-temperature metamorphic rocks in the Archaean Napier Complex, East Antarctica. Ph.D. Thesis of the Graduate University for Advanced Studies, Japan 126 p. (unpublished).
Hokada, T. (2001): Feldspar thermometry in ultrahigh-temperature metamorphic rocks: Evidence of crustal metamorphism attaining ~1100°C in the Archean Napier Complex, East Antarctica. Am. Mineral., **86**, 932–938.
Hokada, T., Osanai, Y., Toyoshima, T., Owada, M., Tsunogae, T. and Crowe, W.A. (1999): Petrology and metamorphism of sapphirine-bearing aluminous gneisses from Tonagh Island in the Napier Complex, East Antarctica. Polar Geosci., **12**, 49–70.
Ishizuka, H., Ishikawa, M., Hokada, T. and Suzuki, S. (1998): Geology of the Mt. Riiser-Larsen area of the Napier Complex, Enderby Land, East Antarctica. Polar Geosci., **11**, 154–171.
Johannes, W. and Holtz, F. (1996): Petrogenesis and Experimental Petrology of Granitic Rocks. Berlin, Springer-Verlag, 335 p.
Motoyoshi, Y. and Shiraishi, K. (1995): Quantitative chemical analyses of rocks with X-ray fluorescence analyzer: (1) Major elements. Nankyoku Shiryô (Antarct. Rec.), **39**, 40–48 (in Japanese with English abstract).
Motoyoshi, Y. and Hensen, B.J. (2001): F-rich phlogopite stability in ultra-high temperature metapelites from the Napier Complex, East Antarctica. Am. Mineral., **86** (in press).
Osanai, Y., Toyoshima, T., Owada, M., Tsunogae, T., Hokada, T., and Crowe, W.A. (1999): Geology of ultrahigh-temperature metamorphic rocks from Tonagh Island in the Napier Complex, East Antarctica. Polar Geosci., **12**, 1–28.
Patiño Douce, A.E. (1997): Generation of metaluminous A-type granites by low-pressure melting of calc-alkaline granitoids. Geology, **25**, 743–746.
Sheraton, J.W., Tingey, R.J., Black, L.P., Offe, L.A. and Ellis, D.J. (1987): Geology of Enderby Land and western Kemp Land, Antarctica. BMR Bull., **223**, 51 p.
Skjerlie, K.P. and Johnston, A.D. (1992): Vapor-absent melting at 10 kbar of a biotite- and amphibole-bearing tonalitic gneiss: implications for the generation of A-type granites. Geology, **20**, 263–266.
Tsunogae, T., Osanai, Y., Toyoshima, T., Owada, M., Hokada, H. and Crowe, W.A. (2000): Fluorine-rich calcic amphiboles in ultrahigh-temperature mafic granulite from Tonagh Island in the Napier Complex, East Antarctica: Preliminary report. Polar Geosci., **13**, 103–113.
Whalen, J.B., Currie, K.L. and Chappell, B.W. (1987): A-type granites: geochemical characteristics, discrimination and petrogenesis. Contrib. Mineral. Petrol., **95**, 407–419.
Whitney, J.A. (1975): The effects of pressure, temperature, and XH2O on phase assemblage in four synthetic rock compositions. J. Geol., **83**, 1–31.
Yoshimura, Y., Motoyoshi, Y., Grew, E.S., Miyamoto, T., Carson, C.J. and Dunkley, D.J. (2000): Ultrahigh-temperature metamorphic rocks from Howard Hills in the Napier Complex, East Antarctica. Polar Geosci., **13**, 60–85.

(Received March 8, 2001; Revised manuscript accepted May 9, 2001)